Title

No circadian clock-gene circuit in the generation of cellular bioluminescence rhythm of *CaMV35S::PtRLUC* in duckweed

Author List

Emiri Watanabe[1,2], Tomoaki Muranaka[1,3], Shunji Nakamura[1,4], Minako Isoda[1], Shogo Ito[1], Tokitaka Oyama[1,*]

*Corresponding author (email): oyama.tokitaka.8w@kyoto-u.ac.jp

Author Affiliation

1. Department of Botany, Graduate School of Science, Kyoto University, Kitashirakawa-Oiwake-cho, Sakyo-ku, Kyoto, 606-8502, Japan

Present addresses

2. Department of Complexity Science and Engineering, Graduate School of Frontier Sciences, The University of Tokyo, Kashiwa, Chiba 277-8561, Japan
3. Faculty of Agriculture, Kagoshima University, Korimoto 21-24-1, Kagoshima, 890-0065, Japan
4. Department of Biological Sciences, Graduate School of Science, The University of Tokyo, Tokyo, 113- 0033, Japan

Summary

The circadian clock is responsible for the temporal regulation of various physiological phenomena in plants. Individual cells contain the cellular circadian clock consisting of the clock gene circuit. Physiological rhythms are coordinated in the plant body in an orderly manner. Multiple circadian rhythms with different free running periods (FRPs) can coexist in the same plant. In addition to different circadian properties between tissues/organs, uncoupled circadian rhythms in the same cell have been reported. The relationship between the cellular circadian clock and the various circadian outputs with different FRPs is currently unknown. Using a dual-color bioluminescence monitoring system in *Lemna minor* transfected with the *AtCCA1::LUC+* and *CaMV35S::PtRLUC* reporters, cellular bioluminescence rhythms with different FRPs were detected in the same cells. Co-transfection experiments with the two reporters and a clock gene overexpressing effector revealed that the circadian properties of the *AtCCA1::LUC+* rhythm, but not those of the *CaMV35S::PtRLUC* rhythm, were altered in the cells with a dysfunctional clock gene circuit. This indicates that the *AtCCA1::LUC+* rhythm is a direct output of the cellular circadian clock while the *CaMV35S::PtRLUC* rhythm is not. After plasmolysis, the *CaMV35S::PtRLUC* rhythm disappeared while the *AtCCA1::LUC+* rhythm persisted. This suggested that *CaMV35S::PtRLUC* is a symplast/apoplast mediated circadian rhythm generated at an organismal level. This idea is consistent with the observation that the phases of *CaMV35S::PtRLUC* cellular rhythms remain highly synchronized while those of *AtCCA1::LUC+* rhythms gradually get desynchronized. The plant circadian system consists of both cell-autonomous rhythms and non-cell-autonomous rhythms that are unaffected by the cellular clock.

Keywords:

circadian rhythms, clock genes, dual-color bioluminescence, *Lemna minor*, luciferases, non-cell-autonomous rhythm, single-cell monitoring

Introduction

Many physiological phenomena in plants show circadian rhythms.[1] The circadian clock is a cell-autonomous system composed of a number of clock genes that form transcription–translation feedback loops (TTFLs).[2,3] In *Arabidopsis*, dawn-expressed *CIRCADIAN CLOCK-ASSOCIATED 1* (*CCA1*), *LATE ELONGATED HYPOCOTYL* (*LHY*), morning-to-evening-expressed *PSEUDO-RESPONSE REGULATOR* (*PRR*) family, evening-to-night-expressed *EARLY FLOWERING 3* (*ELF3*) , *ELF4*, and *LUX ARRHYTHMO* (*LUX*) repress genes expressed during earlier phases. The F-box protein ZEITLUPE (ZTL) affects the TTFLs by temporal promotion of proteasomal degradation of PRR members. Disruption and/or overexpression of these clock genes impairs the circadian rhythm.[2,3] The TTFL oscillator governs the circadian rhythms of various physiological processes in plants, and mutations in clock genes alter these circadian rhythms.[4,5]

Physiological rhythms with different free running periods (FRPs) have been observed in plants.[6] For example, rhythms in cytosolic free calcium (Ca^{2+}) levels have a different FRP from that of *Lhcb* gene expression in tobacco.[7] Differences in the FRPs of bioluminescence rhythms were observed in *Arabidopsis* seedlings expressing a firefly luciferase under circadian promoters *CHALCONE SYNTHASE* (*CHS*), *CHLOROPHYLL A/B BINDING PROTEIN* (*CAB*), *PHYTOCHROME B* (*PHYB*) and *CATALASE 3* (*CAT3*).[8–10] Tissue-specific modulation of the TTFL is considered to be a contributing factor to these different FRPs.[6,11] These distinct oscillators can bring about uncoupled rhythms between tissues/organs and influence the coordination of physiological processes at the organismal level.

In addition to tissue/organ-specific circadian rhythms, intracellular uncoupling of two circadian rhythms has also been reported in plant cells.[12] Bioluminescence of a luciferase driven by a constitutive promoter showed a circadian rhythm in various duckweeds, and *CaMV35S::PtRLUC* (a modified click beetle red color luciferase gene) showed bioluminescence rhythms uncoupled from those of *AtCCA1::LUC+* (a firefly yellow-green luciferase gene) in individual cells in *Lemna minor*.[12,13] The uncoupled rhythms were detected using a dual-color bioluminescence monitoring system at a single-cell level, in which *AtCCA1::LUC+* and *CaMV35S::PtRLUC* reporters were simultaneously transfected into the cells in the duckweed plant by particle bombardment. The intracellular uncoupling was observed as inconsistent phase relation and different FRPs under prolonged and constant light conditions. The *AtCCA1::LUC+* bioluminescence rhythm was shown to be cell-autonomously generated under the control of the TTFL in individual cells, through functional analysis by co-transfecting an effector (overexpression, knockdown and knockout of clock genes) with the circadian reporter.[14–16] In duckweed plants, desynchronization of the cell-autonomous circadian clock occurs between cells in the same tissue under constant conditions, although weak cell-to-cell interaction influencing their phases is expected.[17,18] However, it is unclear how the intracellular uncoupling between *AtCCA1::LUC+* and *CaMV35S::PtRLUC* bioluminescence rhythms happens in individual cells, as the mechanism underlying the *CaMV35S::PtRLUC* bioluminescence rhythm is currently unknown.[12] Cell autonomy and the direct involvement of TTFL are questionable. In this study, we

performed co-transfection using circadian reporters and clock gene overexpressing effectors in a dual-color bioluminescence monitoring system at a single-cell level. We also analyzed the effects of plasmolysis on the cellular circadian rhythms. We show that the *CaMV35S::PtRLUC* bioluminescence rhythm is non-cell-autonomously generated, without direct regulation by the clock-gene circuit.

Results

The period difference between *AtCCA1::LUC+* and *CaMV35S::PtRLUC* bioluminescence rhythms in the same cell

In order to directly compare circadian properties of the bioluminescence rhythms between the two reporters, we performed dual-color bioluminescence monitoring at a single-cell level.[12] Circadian reporters with different luminescence colors, *AtCCA1::LUC+* (yellow-green) and *CaMV35S::PtRLUC* (red), were introduced into *L. minor* cells (epidermal and mesophyll cells) through particle bombardment (Figure 1A). The bioluminescence of individual cells was observed using an EM-CCD camera with a filter exchanger containing green-pass and red-pass filters, and the cellular luminescence intensities of each reporter were reconstructed based on a set of filtered luminescence images (Figure 1B). A set of luminescence images was acquired every hour according to the time schedule shown in Figure 1C.

AtCCA1::LUC+ and *CaMV35S::PtRLUC* bioluminescence rhythms of 37 cells from the same frond under constant light are shown in Figure 2. As shown in Figure 2A and 2B, most cells showed circadian rhythms of both bioluminescence reporters. The FRP and relative amplitude error (RAE) of each luminescence trace were calculated using the fast Fourier transform non-linear least squares (FFT-NLLS) method.[19] The RAE value represents the degree of confidence of rhythmicity, ranging from 0 (complete sine-fitting) to 1 (arrhythmic). In this study, bioluminescence traces with RAE < 0.2 were defined as rhythmic, and the rest were defined as arrhythmic. Every cell showed *CaMV35S::PtRLUC* rhythm, while 33 cells (89%) showed *AtCCA1::LUC+* rhythm (Table S1). Although the bioluminescence traces of *CaMV35S::PtRLUC* in all cells were judged to be rhythmic, the *CaMV35S::PtRLUC* rhythm looked lower in amplitude than the *AtCCA1::LUC+* rhythm (Figure 2A and 2B). FRPs of *AtCCA1::LUC+* and *CaMV35S::PtRLUC* rhythms were distributed differently, with values of 25.5 ± 0.8 h and 24.7 ± 0.6 h, respectively (Figure 2C and Table S1). The FRP of the *CaMV35S::PtRLUC* rhythm was significantly shorter than that of the *AtCCA1::LUC+* rhythm in the same set of cells in a frond (Welch *t*-test, $p=3.8\times10^{-13}$). The shorter FRP of *CaMV35S::PtRLUC* rhythm was also observed in *L. minor* plants that had grown under constant light without experiencing an entrainment dark stimulus.[12]

Figures 2D and 2E show the phase distributions and degrees of synchrony (synchronization index: SI) at t=24 h and 96 h for *AtCCA1::LUC+* rhythms and *CaMV35S::PtRLUC* rhythms, respectively. The SI of *AtCCA1::LUC+* rhythm was 0.96 at t=24 h and decreased to 0.66 at t=96 h. The SI of *CaMV35S::PtRLUC* at t=24 h was 0.85, which was almost the same as that at t=96 h (0.79).

The SI of *AtCCA1::LUC+* rhythm continuously decreased during the constant light condition, while that of *CaMV35S::PtRLUC* rhythm was stable (Figure 2F). Previous studies found that desynchronization of *AtCCA1::LUC+* cellular rhythms occurred under constant light condition in duckweed plants that had been entrained.[17,18] The higher synchrony of *CaMV35S::PtRLUC* cellular rhythms in fronds with asynchronous *AtCCA1::LUC+* cellular rhythms has also been reported in plants that had not experienced entrainment.[12]

In summary, we noted differences in the period and desynchronization behavior between the *AtCCA1::LUC+* and *CaMV35S::PtRLUC* rhythms in the same frond through dual-color bioluminescence monitoring at a single cell level.

<u>Comparison of the *AtCCA1::LUC+* and *CaMV35S::PtRLUC* bioluminescence rhythms among different fronds</u>

In *L. minor* transgenic plants carrying an *AtCCA1::LUC+* reporter, the circadian behaviors of bioluminescence showed a variation among fronds.[18] To investigate variations in cellular circadian behaviors of *AtCCA1::LUC+* and *CaMV35S::PtRLUC* rhythms among fronds, we studied four fronds (including that shown in Figure 2) through dual-color bioluminescence monitoring (dual#1-#4; Table S1) and three fronds for each of the reporters through single reporter bioluminescence monitoring (sCCA1#1-#3, s35S#1-#3; Table S2). The mean FRPs of *AtCCA1::LUC+* rhythm determined by dual-color monitoring were 25.3-27.4 h, and those of *CaMV35S::PtRLUC* rhythm were 24.0-25.0 h (Figure 3A). In three out of the four fronds, the FRPs of *CaMV35S::PtRLUC* rhythm were significantly shorter than those of *AtCCA1::LUC+* rhythm. This was also confirmed by comparing FRPs of the two rhythms in individual cells; 97 out of 116 cells showed shorter FRPs in case of *CaMV35S::PtRLUC* rhythm (Figure 3B). Interestingly, the *CaMV35S::PtRLUC* rhythm (σ^2 = 0.67) showed lower FRP variation between cells than the *AtCCA1::LUC+* rhythm (σ^2 = 2.60) (*F* test, $p = 3.2\times10^{-12}$). The FRP variation is linked to desynchronization of cellular rhythms in a frond.[17] In fact, the SI of *AtCCA1::LUC+* rhythm in each frond continuously decreased while that of *CaMV35S::PtRLUC* was stable (Figure 2F and S1A). These differences in cellular circadian properties between the *AtCCA1::LUC+* and *CaMV35S::PtRLUC* rhythms were confirmed through single reporter bioluminescence monitoring (Table S2, Figure S1BC). With respect to the phase relation, the mean peak phases of the bioluminescence rhythms showed higher variation between fronds in dual-reporter experiments (*AtCCA1::LUC+*, 4.307-5.204 rad; *CaMV35S::PtRLUC*, 0.334-1.890 rad) than those in single reporter experiments (*AtCCA1::LUC+*, 5.284-5.654 rad; *CaMV35S::PtRLUC*, 0.706-1.087 rad) (Tables S1 and S2). The higher phase variation in the dual-reporter experiments might be due to noise amplification in the process of reconstruction for luminescence intensities of both reporters. The differences in the FRPs and the intercellular synchrony between the two bioluminescence rhythms indicate differences in the mechanisms of oscillation generation between them.

160 Robustness of *CaMV35S::PtRLUC* bioluminescence rhythm against clock gene overexpression at
161 the single cell level
162 We co-transfected the overexpressing effector of each of the three *L. minor* clock gene homologs,
163 *LmZTL*, *LmLUX*, and *LmELF3*, with the dual reporters to examine their effects on the *AtCCA1::LUC+*
164 and *CaMV35S::PtRLUC* bioluminescence rhythms in the same cell (Table S1 and Figure S2). In
165 *Arabidopsis*, it was reported that moderate and strong overexpression of *ZTL* caused shortening of
166 FRP and loss of circadian rhythms, respectively.[20] In *L. minor*, *LmZTL* overexpression caused a
167 destabilization of *AtCCA1::LUC+* rhythm (Table S1). When RAE<0.2 was used as a criterion for
168 rhythmic cells, only 21% of the analyzed cells showed circadian rhythms in the experiment dual-
169 ZTLox#1 (Figure 4A and 4C). Without the *CaMV35S::LmZTL* effector, most cells showed
170 *AtCCA1::LUC+* rhythm (Figure 2C and Table S1). This indicated that overexpression of *LmZTL*
171 disrupted the clock gene circuit in the transfected cells. By contrast, overexpression of *LmZTL* did not
172 affect the *CaMV35S::PtRLUC* rhythm in the analyzed cells. Every cell showed a waveform rhythm
173 similar to that observed in experiments without the *CaMV35S::LmZTL* effector (Figures 2B and 4B).
174 The mean FRP was 24.1 ± 0.6 h in the experiment dual-ZTLox#1, which was similar to that without
175 the effector (Table S1). It is noteworthy that *AtCCA1::LUC+* bioluminescence traces in rhythmic cells
176 (RAE<0.2) in case of dual-ZTLox#1 showed a waveform and phase similar to those of the
177 *CaMV35S::PtRLUC* bioluminescence rhythm (Figures 4A and 4B). This *CaMV35S::PtRLUC*-type
178 bioluminescence rhythm exhibited by *AtCCA1::LUC+* was also observed in the single reporter
179 experiment with *LmZTL* overexpression (Figure S3). This indicates that the *AtCCA1::LUC+*
180 transfected cells are capable of producing *CaMV35S*-type bioluminescence rhythm when the clock-
181 gene circuit is disrupted by the overexpression of *LmZTL*. Those cells in which the TTFL oscillator is
182 disrupted may therefore have the potential to produce the *CaMV35S::PtRLUC*-type bioluminescence
183 rhythm with any luciferase reporter in the co-transfection experiments.
184 In transgenic *Arabidopsis* overexpressing *LUX* (*PCL*), dampening of the rhythmic expression
185 of clock-genes has been reported.[21] In *L. minor*, *LmLUX* overexpression shortened the FRP of
186 *AtCCA1::LUC+* rhythm with an amplitude similar to that in the experiment without the effector (Figures
187 4D, 4F and Table S1). By contrast, *LmLUX* overexpression did not affect the *CaMV35S::PtRLUC*
188 rhythm in the analyzed cells. Every cell showed a waveform and FRP similar to those in experiments
189 without the effector (Figures 2D, 4E, 4F and Table S1). Consequently, *LmLUX* overexpression
190 shortened the FRPs of the *AtCCA1::LUC+* rhythm compared with those of the *CaMV35S::PtRLUC*
191 rhythm in most of the analyzed cells (Figures S2 and S4). This indicated that *LmLUX* overexpression
192 disrupted the clock gene circuit in the transfected cells without affecting the *CaMV35S::PtRLUC*
193 rhythm.
194 Overexpression of *LgELF3* in the cells of *Lemna gibba* resulted in perturbation of light
195 entrainment, and an increase in the number of cells with unstable rhythms and longer FRPs.[16] In *L.*
196 *minor*, overexpression of *LmELF3* caused unstable *AtCCA1::LUC+* cellular rhythms and longer FRPs
197 in dual-reporter experiments (Figure 4G, 4I and Table S1). By contrast, cellular *CaMV35S::PtRLUC*

198 bioluminescence showed a stable rhythm and no alteration of FRP (Figure 4H, 4I and Table S1). This
199 indicated that overexpression of *LmELF3* modified the clock gene circuit in the transfected cells
200 without affecting the *CaMV35S::PtRLUC* rhythm. In single-reporter experiments, many cells co-
201 transfected with *LmELF3* overexpressing effector showed unstable *AtCCA1::LUC*+ rhythm but stable
202 *CaMV35S::PtRLUC* rhythm (Table S2). These results suggested that *LmELF3* overexpression
203 impaired the clock gene circuit in the transfected cells that maintained the *CaMV35S::PtRLUC* rhythm.
204 Results of the overexpression of the three clock genes, therefore, indicate that the
205 *CaMV35S::PtRLUC* bioluminescence rhythm is generated on a cellular level without direct regulation
206 by the clock gene circuit in the same cell.
207
208 Disruption of the *CaMV35S::PtRLUC* bioluminescence rhythm in a hypertonic medium
209 While the co-transfection of a clock-gene overexpressing effector affects the circadian clock in the
210 luciferase-expressing cells, most cells not transfected by particle bombardment are unlikely to be
211 affected by the effector. Therefore, it raises the possibility that the *CaMV35S::PtRLUC* rhythm in the
212 transfected cells is supported by surrounding tissues with normal circadian rhythms. In order to disrupt
213 the intercellular signal transmission to the transfected cells, we exposed the frond to hypertonic
214 medium to cause plasmolysis. We performed dual-color monitoring experiment on the fronds being
215 subjected to NF medium with 500 mM mannitol (Figure 5). Plasmolysis of cells that were transfected
216 with *CaMV35S::GFP-h* by particle bombardment was confirmed in the frond that was subjected to the
217 hypertonic medium (Figure S5). The *AtCCA1::LUC*+ rhythm was observed in all analyzed cells in
218 hypertonic conditions, although a period lengthening appeared (Figure 5A, 5C and Table S1).
219 Interestingly though, the *CaMV35S::PtRLUC* rhythm disappeared in the same cells (Figure 5B, 5C
220 and Table S1). Similar results were obtained for the circadian rhythmicity of each reporter in the single
221 reporter experiments involving hypertonic treatment (Tables S2). The disappearance of the
222 *CaMV35S::PtRLUC* rhythm in cells showing stable *AtCCA1::LUC*+ rhythm strongly suggests that the
223 *CaMV35S::PtRLUC* rhythm is non-cell-autonomously generated with the support of surrounding
224 tissues.
225
226
227 **Discussion**
228 In this study, we have demonstrated that the *CaMV35S::PtRLUC* bioluminescence rhythm is not
229 governed by the clock gene circuit in the expressing cells but requires the support of surrounding
230 tissues in the plant. The maintenance of high synchrony in the *CaMV35S::PtRLUC* rhythm between
231 cells in the frond stands in contrast to the dyssynchronous nature of the *AtCCA1::LUC*+ rhythm, that
232 is linked to the clock gene circuit (Figure 2F).[17] This indicates distinct characteristics of cell-
233 autonomous and non-cell-autonomous rhythms. Figure 6 shows a conceptual framework of
234 generation of these rhythms in individual cells in the plant. In each cell, TTFL drives the cell-
235 autonomous rhythms such as the *AtCCA1::LUC*+ rhythm. The non-cell-autonomous rhythms such as

236 the *CaMV35S::PtRLUC* rhythm are driven by symplast/apoplast mediation. Circadian rhythms that
237 are driven by changes in concentrations of ions and small molecules and the water flux potentially
238 belong to this category. Circadian-regulated solute transporters of individual cells appear to generate
239 these circadian rhythms,[22] while changes in the concentrations of these diffusive elements inevitably
240 involve extracellular factors that are shared by the plant cells. These non-cell-autonomous rhythms
241 can be driven at an organismal level. The rhythmicity at the organismal level depends on the
242 integration of temporal information between cellular clocks. Therefore, a certain degree of synchrony
243 between them is required to generate the non-cell-autonomous rhythms. This framework effectively
244 explains the distinct characteristics of the *AtCCA1::LUC+* and *CaMV35S::PtRLUC* rhythms. Diffusive
245 elements such as luciferin, magnesium ions, protons, ATP, and oxygen that influence the luciferase
246 enzyme activity[23] may oscillate in a circadian manner in duckweed. In fact, a circadian rhythm of the
247 absorption of ions such as potassium and magnesium ions, has been reported in the duckweed
248 species *Lemna gibba*.[24,25] The circadian rhythm at an organismal level should show higher synchrony
249 between cells than the cell-autonomous rhythm. Thus, the *CaMV35S::PtRLUC* rhythm can be more
250 synchronous than the *AtCCA1::LUC+* rhythm in a frond. Notably the *CaMV35S::PtRLUC* rhythm is
251 lost or is rendered unstable in a frond with cellular clocks in an asynchronous state.[12]
252 An important finding of this study is that physiological rhythms in individual cells are not
253 always governed by their own cellular circadian clocks. These rhythms can stay stable in the plant
254 even when the synchrony between the cellular clocks of its cells becomes low. This allows imprecision
255 of individual cellular clocks and uneven circadian properties between cells. Indeed, in a *L. gibba* frond
256 under constant light, each cellular clock showed an unstable FRP (SD for cycle-to-cycle variation:
257 2.45 h) and a relatively large variation of FRP was reported between cells (SD 1.11 h).[17] The highly
258 synchronous rhythm independent of the quality of individual cellular clocks would effectively work
259 without the need to maintain the accuracy of each clock.
260 Our results clearly indicate that the *CaMV35S::PtRLUC* rhythm was maintained in the cells
261 in which the *AtCCA1::LUC+* rhythm was disrupted by *ZTL* overexpression. This strongly suggests
262 that the clock gene circuit is dispensable for the *CaMV35S::PtRLUC* rhythm in the cell. This does not
263 necessarily mean that the gene circuit of the plant cells is completely dispensable for the
264 *CaMV35S::PtRLUC* rhythm. The *ZTL* overexpression after transfection using particle bombardment
265 was expected to disrupt the gene circuit only in the transfected cells, and most cells in the plant were
266 not affected. These unaffected cells were probably responsible for the non-cell-autonomous rhythm
267 at an organismal level. The stable transformation method has been established for *L. minor*,[18,26] and
268 transgenic plants overexpressing *ZTL* would be an interesting model for studying the necessity of the
269 clock gene circuit for the *CaMV35S::PtRLUC* rhythm. In a previous study, the circadian rhythms of
270 bioluminescence reporters in roots (rootstocks) of *Arabidopsis* clock mutants were partially restored
271 by grafting wild type shoot apex.[27] In that case, it appears that the cellular circadian clock in the roots
272 was restored. Therefore, the mechanism for generating the rhythm in *Arabidopsis* may differ from that

273 of the *CaMV35S::PtRLUC* rhythm in duckweed. In fact, multiple mechanisms may exist to generate
274 non-cell-autonomous circadian rhythms in plants.
275 Intercellular communication is an interesting aspect of the plant circadian system.[11,28]
276 Synchronization between neighboring cellular clocks and long-distance clock communication have
277 been previously reported.[17,18,27,29–33] A non-cell-autonomous physiological rhythm with a high spatial
278 synchrony can effectively function in the synchronization process between cellular clocks if the clock
279 gene circuit is affected by the physiological rhythm in individual cells. Calcium is a potential mediator
280 of this intercellular communication because cytosolic free calcium in plant cells is a physiological
281 circadian output and is also involved in the regulation of the circadian clock.[34,35] Interestingly, it has
282 been suggested that the calcium rhythm and the *Cab* (*Lhcb*) gene expression rhythm are separately
283 controlled for the determination of their FRPs and the oscillation generation by the clock gene circuit.[5,7]
284 It is therefore worth investigating whether the calcium rhythm is non-cell-autonomous.
285 The mechanisms that generate the *CaMV35S::PtRLUC* bioluminescence rhythm are
286 currently unknown.[12] In the conceptual framework (Figure 6), physiological conditions associated with
287 the bioluminescence reaction in the cells seem to post-transcriptionally mediate the rhythm. Circadian
288 rhythms in the levels of ions and/or metabolites at an organismal level may bring about the
289 bioluminescence rhythm.[22,28,36] These rhythms may not be the simple sum of the individual cellular
290 rhythms in the plant because the FRP of the *CaMV35S::PtRLUC* rhythm is different from that of the
291 *AtCCA1::LUC+* rhythm (Table S1). Further studies of such non-cell-autonomous rhythms should
292 improve the understanding the circadian systems in plants, which involve various cells with cell-
293 autonomous circadian clocks.
294
295
296 **Materials and Methods**
297 Plant material and growth conditions
298 *Lemna minor* 5512 was maintained in NF medium with 1% sucrose under constant light conditions in
299 a temperature-controlled room (25 ± 1 °C), as previously described.[13] The white light (~20 μE m^{-2} s^{-}
300 ^{1}) was generated by fluorescent lamps (FLR40SEX-W/M/36-HG, NE, Japan). Plants were grown on
301 60 ml of the medium in 200-ml Erlenmeyer flasks plugged with cotton. New stock cultures were made
302 weekly, and well-grown plants were used for the experiments. To entrain the circadian rhythm, plants
303 were cultured under at least three 12 h light/12 h dark cycles in an incubator (MIR-153, Panasonic,
304 Japan) before starting the experiments.
305
306 Luciferase reporters
307 As circadian bioluminescent reporters, we used *pUC-AtCCA1::intron-LUC+* (*AtCCA1::LUC+*), and
308 *pUC18-CaMV35S::PtRLUC* (*CaMV35S::PtRLUC*), which have been described previously[12]. PtRLUC
309 is a red-shift mutant (S246H/H347A) of Emerald luciferase (ELuc) from Brazilian click beetle
310 (*Pyrearinus termitilluminans*).[37]

311

312 Clock-gene overexpression effectors

313 *pUC18-CaMV35S::LmZTL*, *pUC18-CaMV35S::LmLUX*, and *pUC18-CaMV35S::LmELF3* were
314 constructed as follows. Coding regions of *LmZTL*, *LmLUX*, and *LmELF3* from *Lemna minor* 5512
315 were amplified using PCR with the following primer sets:
316 CgcggccgcCACCATGGAGTGGAATAGTGATTCG and CggcgcgccTTAAATGAGCTCCGAGAAGCC
317 for *LmZTL*, CgcggccgcATGGCGGACGGTGATGGCGG and
318 CggcgcgccTTATTTGTAACCGGGAGAAACATGG for *LmLUX*,
319 CgcggccgcATGAAGAGAGGGAGAGAGGAAGATAAG and
320 CggcgcgccCTACAGCGGATCGTATCCCTG for *LmELF3*. Primer sequences for each gene were
321 designed based on the genome sequence of *Lemna minor* 5500.[38] The small-letter 8-b sequence in
322 each primer sequence represents a restriction enzyme recognition site (*Not*1 for forward primer and
323 *Asc*1 for reverse primer). cDNA that was synthesized from total RNA of *L. minor* 5512 using ReverTra
324 Ace (TOYOBO, Japan) was used as the template for the PCR. The total RNA was extracted from the
325 whole plant using NucleoSpin RNA (Takara, Japan). The amino acid sequences of LmZTL and
326 LmELF3 are identical in the strains 5500 and 5512. Compared with the strain 5500, the amino acid
327 sequence of LmLUX in strain 5512 contains four amino acid substitutions and an insertion of two
328 amino acids. The amplicon of each gene was cloned into *pENTR-D-TOPO* (Invitrogen, MA, USA) with
329 an additional multi-cloning site. Using the LR reaction, the coding region in this plasmid was integrated
330 into *pUC18-CaMV35S-attR1-attR2-NosT*, in which the *att*R1-*att*R2 sequence (Invitrogen) was located
331 between the *CaMV35S* promoter and the Nos terminator.

332

333 Particle bombardment and bioluminescence monitoring

334 Reporter constructs were introduced into *L. minor* plants by particle bombardment as described
335 previously.[13] In both single- and dual-reporter experiments, the amounts of plasmid DNA coding for
336 *AtCCA1::LUC+* and *CaMV35S::PtRLUC*, were 2 μg, and 0.2 μg, respectively. In co-transfection
337 experiments, 1 μg overexpression effector of a clock gene was added to the reporter(s).
338 Dual-color bioluminescence monitoring at a single cell level was carried out as described previously.[12]
339 In short, the imaging system consisted of an EM-CCD camera (ImagEM C9100-13; Hamamatsu
340 Photonics, Japan) with a lens (VS-50085/C 0.85/50mm; VS Technology, Japan), a handmade filter
341 changer with a rotation motor (ARS-4036-GM; Chuo Precision Industrial Co., Japan), a handmade
342 motor-driven stage with rotation and z-axis stages (ARS-6036-GM and ALV-902-HP; Chuo Precision
343 Industrial Co., Japan), and an illuminating system with an end-emitting fiber optics guiding LED white
344 light (approximately 30 μE m^{-2} s^{-1}; RFB2-20SW; CCS Inc, Japan). These devises were set in a
345 lightproof box in an incubator (25 ± 1°C). A green-pass filter (PB0530/080; ⌀49.7 mm; Asahi Spectra,
346 Japan) and red-pass filter (PB0630/040; ⌀49.7 mm; Asahi Spectra) were placed in slots in the filter
347 changer, and one slot was left empty to capture unfiltered images. By controlling this imaging system
348 using PC software (HOKAWO; Hamamatsu Photonics), a series of bioluminescence images for a

349 sample dish were automatically captured every 1 h. Based on the intensities of the filtered
350 bioluminescence of a luminous cell expressing both the reporters, the bioluminescence intensity of
351 each reporter at every time point was calculated. The same imaging protocol was used for single-
352 reporter experiments.
353 Bioluminescence monitoring in the hypertonic conditions (NF medium with 1% sucrose and 500 mM
354 mannitol) was carried out using a plant that was transferred from the normal medium conditions just
355 before the start of the monitoring.
356
357 Fluorescence imaging
358 A fluorescent reporter (*CaMV35S::GFP-h*)[39] was transfected into the duckweed plants, and GFP
359 fluorescence-positive cells were observed under a confocal microscope (LSM510-META; Carl Zeiss,
360 https://www.zeiss.com) as described previously.[40]
361
362 Time series analysis
363 The criteria for luminous spots that were used for time series analysis were the same as those
364 previously described, except for a change in the lower limit of the ratio of luminescence intensities of
365 a 24 h moving average between *AtCCA1::LUC+* and *CaMV35S::PtRLUC* (from 1/20 to 1/100).[12] The
366 FRPs and RAEs of the bioluminescence traces were estimated using the fast Fourier transform non-
367 linear least squares method, as described previously.[12] The peak times of bioluminescence traces
368 were estimated by local quadratic curve fitting, as described previously.[12]
369 Phase $\theta(t)$ of the bioluminescence rhythms $x(t)$ was defined as follows

370 $$\theta(t) = 2\pi \frac{t - t_p^k}{t_p^{k+1} - t_p^k} \ (t^k \leq t < t^{k+1}, k = 1 \ldots M)$$

371 where t_p^k represents the occurrence time of the kth peak of $x(t)$ and M represents the total
372 number of peaks. Data analysis codes are available at https://github.com/ukikusa/circadian_analysis
373
374 Synchronization index
375 To assess the synchrony between cellular rhythms within a plant, the SI, which is known as the order
376 parameter in the Kuramoto model, was calculated at each time point as follows

377 $$R(t) = \frac{1}{N} \left| \sum_k exp(i\theta_k(t)) \right|$$

378 where $\theta_k(t)$ is the phase of the kth cell at time t, and N is the number of cells.
379 The SI at a given time was calculated if the ratio of cells of which the phase was defined was more
380 than 80% of rhythmic cells. For dual reporter experiments, cells showing both rhythms were analyzed.
381
382
383 **References**
384 1. Sweeney, B.M. (1987). Rhythmic phenomena in plants 2nd ed. (Academic Press).

385 2. Nohales, M.A., and Kay, S.A. (2016). Molecular mechanisms at the core of the plant circadian
386 oscillator. Nature Structural & Molecular Biology *23*, 1061–1069.
387 3. Sanchez, S.E., Rugnone, M.L., and Kay, S.A. (2020). Light perception: a matter of time.
388 Molecular Plant *13*, 363–385.
389 4. Somers, D.E., Webb, A.A.R., Pearson, M., and Kay, S.A. (1998). The short-period mutant,
390 toc1-1, alters circadian clock regulation of multiple outputs throughout development in *Arabidopsis*
391 *thaliana*. Development *125*, 10.
392 5. Xu, X., Hotta, C.T., Dodd, A.N., Love, J., Sharrock, R., Lee, Y.W., Xie, Q., Johnson, C.H.,
393 and Webb, A.A.R. (2007). Distinct light and clock modulation of cytosolic free Ca2+ oscillations and
394 rhythmic CHLOROPHYLL A/B BINDING PROTEIN2 promoter activity in Arabidopsis. The Plant Cell
395 *19*, 3474–3490.
396 6. Nohales, M.A. (2021). Spatial organization and coordination of the plant circadian system.
397 Genes *12*, 442.
398 7. Sai, J., and Johnson, C.H. (1999). Different circadian oscillators control Ca^{2+} fluxes and *lhcb*
399 gene expression. Proc Natl Acad Sci U S A *96*, 11659–11663.
400 8. Thain, S.C., Murtas, G., Lynn, J.R., McGrath, R.B., and Millar, A.J. (2002). The circadian
401 clock that controls gene expression in Arabidopsis is tissue specific. Plant Physiology *130*, 102–110.
402 9. Hall, A., Kozma-Bognár, L., Bastow, R.M., Nagy, F., and Millar, A.J. (2002). Distinct
403 regulation of *CAB* and *PHYB* gene expression by similar circadian clocks. The Plant Journal *32*, 529–
404 537.
405 10. Michael, T.P., Salomé, P.A., and McClung, C.R. (2003). Two *Arabidopsis* circadian
406 oscillators can be distinguished by differential temperature sensitivity. PNAS *100*, 6878–6883.
407 11. McClung, C.R. (2019). The plant circadian oscillator. Biology *8*, 14.
408 12. Watanabe, E., Isoda, M., Muranaka, T., Ito, S., and Oyama, T. (2021). Detection of
409 uncoupled circadian rhythms in individual cells of *Lemna minor* using a dual-color bioluminescence
410 monitoring system. Plant and Cell Physiology.
411 13. Muranaka, T., Okada, M., Yomo, J., Kubota, S., and Oyama, T. (2015). Characterisation of
412 circadian rhythms of various duckweeds. Plant Biology *17*, 66–74.
413 14. Miwa, K., Serikawa, M., Suzuki, S., Kondo, T., and Oyama, T. (2006). Conserved expression
414 profiles of circadian clock-related genes in two *Lemna* species showing long-day and short-day
415 photoperiodic flowering responses. Plant Cell Physiol *47*, 601–612.
416 15. Serikawa, M., Miwa, K., Kondo, T., and Oyama, T. (2008). Functional conservation of clock-
417 related genes in flowering plants: overexpression and RNA interference analyses of the circadian
418 rhythm in the monocotyledon *Lemna gibba*. Plant Physiology *146*, 1952–1963.
419 16. Okada, M., Muranaka, T., Ito, S., and Oyama, T. (2017). Synchrony of plant cellular circadian
420 clocks with heterogeneous properties under light/dark cycles. Sci Rep *7*, 317.
421 17. Muranaka, T., and Oyama, T. (2016). Heterogeneity of cellular circadian clocks in intact
422 plants and its correction under light-dark cycles. Sci Adv *2*.

423 18. Ueno, K., Ito, S., and Oyama, T. (2021). An endogenous basis for synchronization manners
424 of the circadian rhythm in proliferating *Lemna minor* plants.
425 19. Plautz, J.D., Straume, M., Stanewsky, R., Jamison, C.F., Brandes, C., Dowse, H.B., Hall,
426 J.C., and Kay, S.A. (1997). Quantitative analysis of <i>Drosophila period<i> gene transcription in
427 living animals. J Biol Rhythms *12*, 204–217.
428 20. Somers, D.E., Kim, W.-Y., and Geng, R. (2004). The F-box protein ZEITLUPE confers
429 dosage-dependent control on the circadian clock, photomorphogenesis, and flowering time. Plant Cell
430 *16*, 769–782.
431 21. Onai, K., and Ishiura, M. (2005). PHYTOCLOCK 1 encoding a novel GARP protein essential
432 for the *Arabidopsis* circadian clock. Genes to Cells *10*, 963–972.
433 22. Haydon, M.J., Bell, L.J., and Webb, A.A.R. (2011). Interactions between plant circadian
434 clocks and solute transport. J Exp Bot *62*, 2333–2348.
435 23. Van Leeuwen, W., Hagendoorn, M.J.M., Ruttink, T., Van Poecke, R., Van Der Plas, L.H.W.,
436 and Van Der Krol, A.R. (2000). The use of the luciferase reporter system forin planta gene expression
437 studies. Plant Mol Biol Rep *18*, 143–144.
438 24. Kondo, T., and Tsudzuki, T. (1978). Rhythm in potassium uptake by a duckweed, *Lemna*
439 *gibba* G3. Plant Cell Physiol *19*, 1465–1473.
440 25. Kondo, T. (1983). Phase shifts of potassium uptake rhythm in *Lemna gibba* G3 due to light,
441 dark or temperature pulses. Plant Cell Physiol *24*, 659–665.
442 26. Chhabra, G., Chaudhary, D., Sainger, M., and Jaiwal, P.K. (2011). Genetic transformation of
443 Indian isolate of Lemna minor mediated by Agrobacterium tumefaciens and recovery of transgenic
444 plants. Physiol Mol Biol Plants *17*, 129–136.
445 27. Takahashi, N., Hirata, Y., Aihara, K., and Mas, P. (2015). A hierarchical multi-oscillator
446 network orchestrates the *Arabidopsis* circadian system. Cell *163*, 148–159.
447 28. Sorkin, M.L., and Nusinow, D.A. (2021). Time will tell: intercellular communication in the plant
448 clock. Trends in Plant Science *26*, 706–719.
449 29. Fukuda, H., Nakamichi, N., Hisatsune, M., Murase, H., and Mizuno, T. (2007).
450 Synchronization of plant circadian oscillators with a phase delay effect of the vein network. Phys. Rev.
451 Lett. *99*, 098102.
452 30. Fukuda, H., Ukai, K., and Oyama, T. (2012). Self-arrangement of cellular circadian rhythms
453 through phase-resetting in plant roots. Phys. Rev. E *86*, 041917.
454 31. Wenden, B., Toner, D.L.K., Hodge, S.K., Grima, R., and Millar, A.J. (2012). Spontaneous
455 spatiotemporal waves of gene expression from biological clocks in the leaf. PNAS *109*, 6757–6762.
456 32. Endo, M., Shimizu, H., Nohales, M.A., Araki, T., and Kay, S.A. (2014). Tissue-specific clocks
457 in Arabidopsis show asymmetric coupling. Nature *515*, 419–422.
458 33. Gould, P.D., Domijan, M., Greenwood, M., Tokuda, I.T., Rees, H., Kozma-Bognar, L., Hall,
459 A.J., and Locke, J.C. (2018). Coordination of robust single cell rhythms in the *Arabidopsis* circadian
460 clock via spatial waves of gene expression. eLife *7*.

34. Johnson, C.H., Knight, M.R., Kondo, T., Masson, P., Sedbrook, J., Haley, A., and Trewavas, A. (1995). Circadian oscillations of cytosolic and chloroplastic free calcium in plants. Science *269*, 1863–1865.

35. Martí Ruiz, M.C., Hubbard, K.E., Gardner, M.J., Jung, H.J., Aubry, S., Hotta, C.T., Mohd-Noh, N.I., Robertson, F.C., Hearn, T.J., Tsai, Y.-C., et al. (2018). Circadian oscillations of cytosolic free calcium regulate the Arabidopsis circadian clock. Nature Plants *4*, 690–698.

36. Haydon, M.J., Mielczarek, O., Robertson, F.C., Hubbard, K.E., and Webb, A.A.R. (2013). Photosynthetic entrainment of the Arabidopsis thaliana circadian clock. Nature *502*, 689–692.

37. Nishiguchi, T., Yamada, T., Nasu, Y., Ito, M., Yoshimura, H., and Ozawa, T. (2015). Development of red-shifted mutants derived from luciferase of Brazilian click beetle *Pyrearinus termitilluminans*. JBO *20*, 101205.

38. Van Hoeck, A., Horemans, N., Monsieurs, P., Cao, H.X., Vandenhove, H., and Blust, R. (2015). The first draft genome of the aquatic model plant *Lemna minor* opens the route for future stress physiology research and biotechnological applications. Biotechnology for Biofuels *8*, 188.

39. Nakano, R.T., Matsushima, R., Ueda, H., Tamura, K., Shimada, T., Li, L., Hayashi, Y., Kondo, M., Nishimura, M., and Hara-Nishimura, I. (2009). GNOM-LIKE1/ERMO1 and SEC24a/ERMO2 are required for maintenance of endoplasmic reticulum morphology in *Arabidopsis thaliana*. The Plant Cell *21*, 3672–3685.

40. Muranaka, T., Kubota, S., and Oyama, T. (2013). A single-cell bioluminescence imaging system for monitoring cellular gene expression in a plant body. Plant and Cell Physiology *54*, 2085–2093.

Acknowledgements

We thank Dr. Hiroshi Kori for fruitful discussions and useful advice. This research was supported by the Japan Society for the Promotion of Science KAKENHI [grant numbers JP21J23250 (E.W.), JP19J23441(S.N.), JP16H06864 (T.M.), JP20K06342 (S.I.), JP17KT0022 (T.O.) and JP19H03245(T.O.)], Japan Science and Technology Agency (JST), JST ALCA (JPMJAL1108, T.O.), and JST SATREPS (JPMJSA2004, T.M., S.I., T.O.).

Author contributions

E.W., T.M. and T.O. designed the study. E.W. and T.O. wrote the manuscript. E.W. performed the bioluminescence monitoring experiments and data analysis. S.N. performed plasmolysis. S.I. and M.I. performed molecular cloning. All authors have contributed to the text.

Declaration of interests

The authors declare no competing interests.

Figure 1

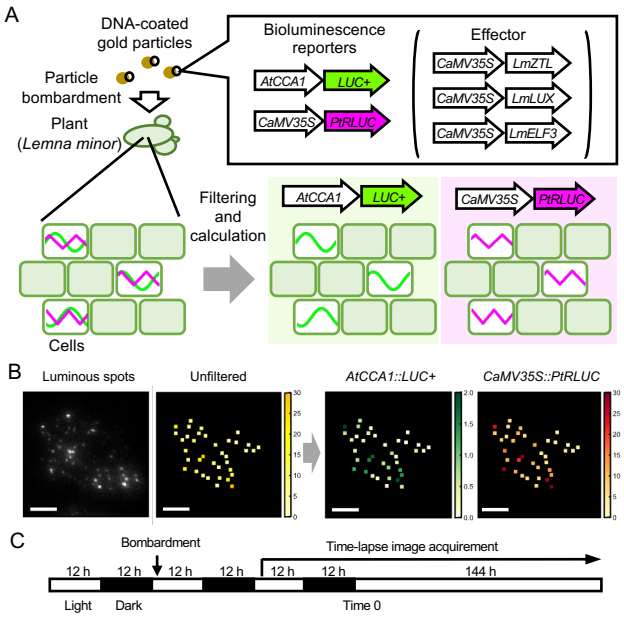

Figure 1. Outline of the dual-color bioluminescence monitoring experiments
(A) Schematic drawing of the measurement of *AtCCA1::LUC+* and *CaMV35S::PtRLUC* bioluminescence at a single-cell level. Bioluminescence reporters were introduced into *Lemna minor* cells by particle bombardment. Filtered cellular bioluminescence was imaged and used for the calculation of luminescence intensities of each reporter. For overexpression experiments, an effector (*CaMV35S::LmZTL*, *CaMV35S::LmLUX* or *CaMV35S::LmELF3*) was co-transfected with the reporters. (B) An example of the reconstruction of cellular luminescence intensities [1000 photons/s] of each reporter. Luminescence intensities of individual cells are color coded. Scale bars are 1 mm. (C) Time schedule of the monitoring experiments. *L. minor* plants that had been cultured under 12 h light 12 h dark cycles were transfected by particle bombardment. The transfected plants were further cultured under 12 h light 12 h dark cycles, and then transferred to the imaging system. Open and closed boxes represent light and dark conditions, respectively. Time 0 is defined as the start of constant light during the time-lapse imaging.

Figure 2

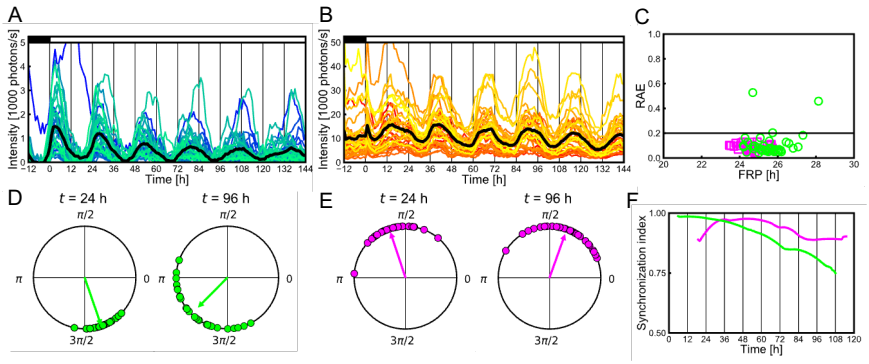

Figure 2. Cellular circadian properties of *AtCCA1::LUC+* and *CaMV35S::PtRLUC* rhythms in the dual-reporter experiment

A total of 37 cells in a frond were analyzed. (A and B) Cellular *AtCCA1::LUC+* (A) and *CaMV35S::PtRLUC* (B) bioluminescence rhythms. The black line represents mean luminescence intensities. Close and open boxes represent light and dark conditions, respectively. (C) The free-running periods (FRPs) and the relative amplitude errors (RAEs) of individual cellular rhythms. Green circles and magenta squares represent *AtCCA1::LUC+* and *CaMV35S::PtRLUC*, rhythms, respectively. Cellular bioluminescence traces with RAE < 0.2 are defined as rhythmic. (D and E) Plots of the phases of *AtCCA1::LUC+* rhythm (D) and *CaMV35S::PtRLUC* rhythm (E) on the unit circle at 24 h and 96 h, respectively. The peak right before 24 h or 96 h is referred to as phase 0 [rad]. The vector represents the vector mean of each plot on the unit circle. The vector length and the angle represent the synchronization index (SI) and a representative phase, respectively, at each time. (F) Temporal changes in the SIs of *AtCCA1::LUC+* (green) and *CaMV35S::PtRLUC* (magenta) rhythms.

Figure 3

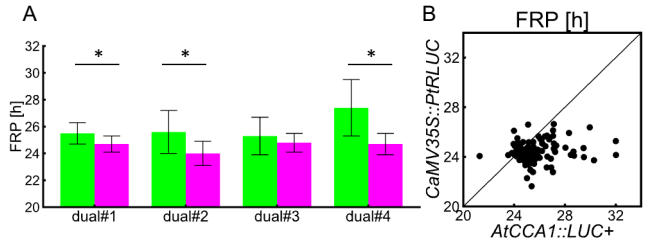

Figure 3 Difference in the free running periods (FRPs) between *AtCCA1::LUC+* and *CaMV35S::PtRLUC* bioluminescence rhythms

Cellular rhythms detected in the four experiments (dual#1: 33 cells, dual#2: 50 cells, dual#3: 18 cells, dual#4: 15 cells) were analyzed. (A) FRPs of *AtCCA1::LUC+* or *CaMV35S::PtRLUC* rhythms in each experiment. Data are expressed as mean ± SD. Asterisk denotes statistically significant difference (Welch's *t* test, $p < 0.01$). (B) A scatterplot of the FRPs between *AtCCA1::LUC+* and *CaMV35S::PtRLUC* rhythms. FRPs of the 116 cells showing the circadian rhythms of both reporters in the four experiments are plotted. The dashed line represents where the FRPs are identical in both rhythms.

Figure 4

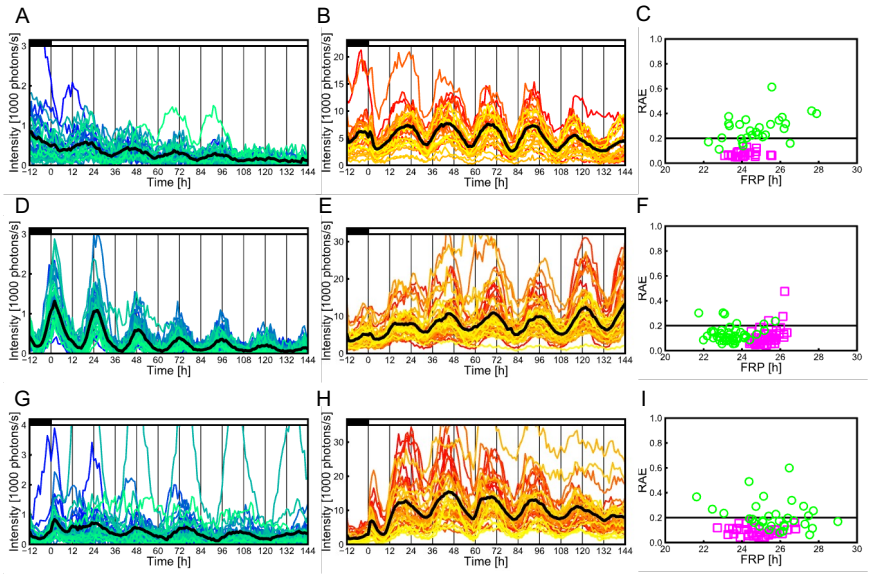

Figure 4. Cellular circadian properties of *AtCCA1::LUC+* and *CaMV35S::PtRLUC* bioluminescence traces in clock-gene overexpression experiments
CaMV35S::LmZTL (dual-ZTLox#1, 29 cells) (A, B, C), *CaMV35S::LmLUX* (dual-LUXox#1, 48 cells) (D, E, F) and *CaMV35S::LmELF3* (dual-ELF3ox#1, 38 cells) (G, H, I) were co-transfected with the dual-color reporters. Cellular *AtCCA1::LUC+* (A, D, G) and *CaMV35S::PtRLUC* (B, E, H) bioluminescence traces are lined in color and a black line in each panel represents mean luminescence intensities. Close and open boxes represent light and dark conditions, respectively. (C, F, I) The free-running periods (FRPs) and the relative amplitude errors (RAEs) of individual cellular rhythms. Green circles and magenta squares represent *AtCCA1::LUC+* and *CaMV35S::PtRLUC* bioluminescence traces, respectively. Cellular bioluminescence traces with RAE < 0.2 are defined as rhythmic.

Figure 5

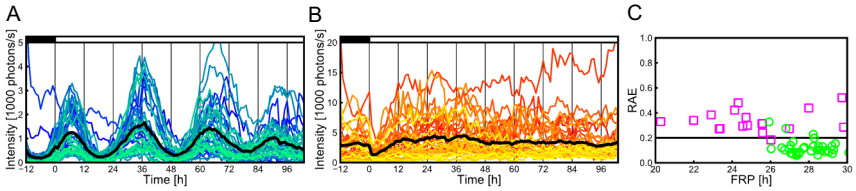

Figure 5. Cellular circadian properties of *AtCCA1::LUC+* and *CaMV35S::PtRLUC* bioluminescence traces in a plant in hypertonic medium

A total of 30 cells in a frond on a hypertonic medium were analyzed for the dual-color reporters. (A and B) Cellular *AtCCA1::LUC+* (A) and *CaMV35S::PtRLUC* (B) bioluminescence traces. A black line represents mean luminescence intensities. Close and open boxes represent light and dark conditions, respectively. (C) Free running periods (FRPs) and the relative amplitude errors (RAEs) of individual cellular rhythms. Green circles and magenta squares represent *AtCCA1::LUC+* and *CaMV35S::PtRLUC* bioluminescence traces, respectively. Cellular bioluminescence traces with RAE < 0.2 are defined as rhythmic.

Figure 6

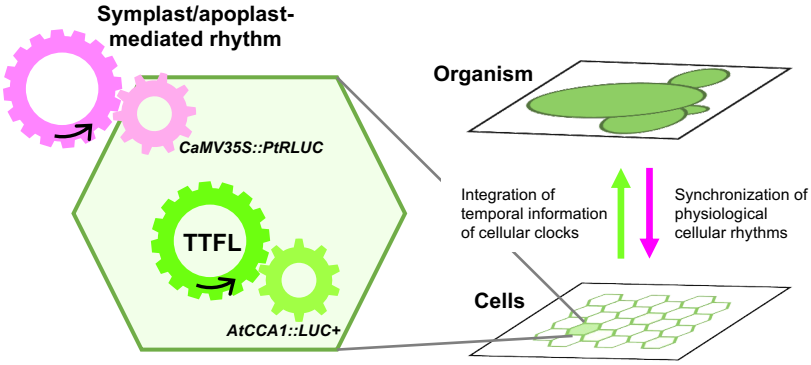

Figure 6. Conceptual framework of the generation of *AtCCA1::LUC+* and *CaMV35S::PtRLUC* bioluminescence rhythms

The *AtCCA1::LUC+* bioluminescence rhythm is generated by the TTFLs in individual cells. The *CaMV35S::PtRLUC* bioluminescence rhythm is a symplast/apoplast-mediated rhythm. Temporal information of cellular clocks is integrated to generate physiological symplast/apoplast-mediated rhythms at an organismal level. These physiological rhythms are synchronous between cells.

Figure S1

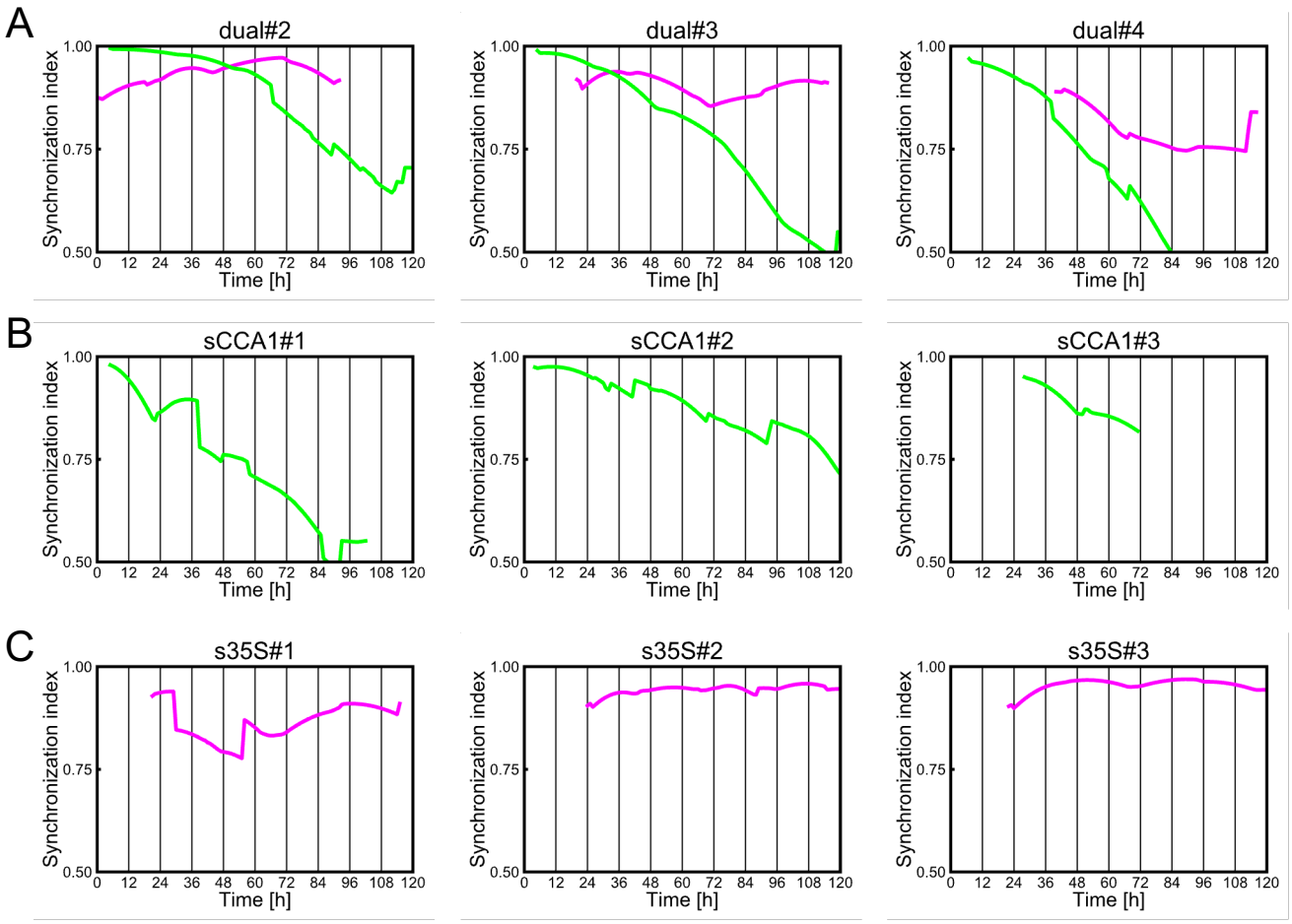

Figure S1. Temporal changes in the synchronization index (SI) of *AtCCA1::LUC+* (green) and *CaMV35S::PtRLUC* (magenta) rhythms in dual and single reporter experiments
(A) Dual-reporter experiments (dual#2-#4), (B) Single-reporter experiments for the *AtCCA1::LUC+* rhythm (sCCA1#1-#3), (C) Single-reporter experiments for the *CaMV35S::PtRLUC* rhythm (s35S#1-#3).

Figure S2

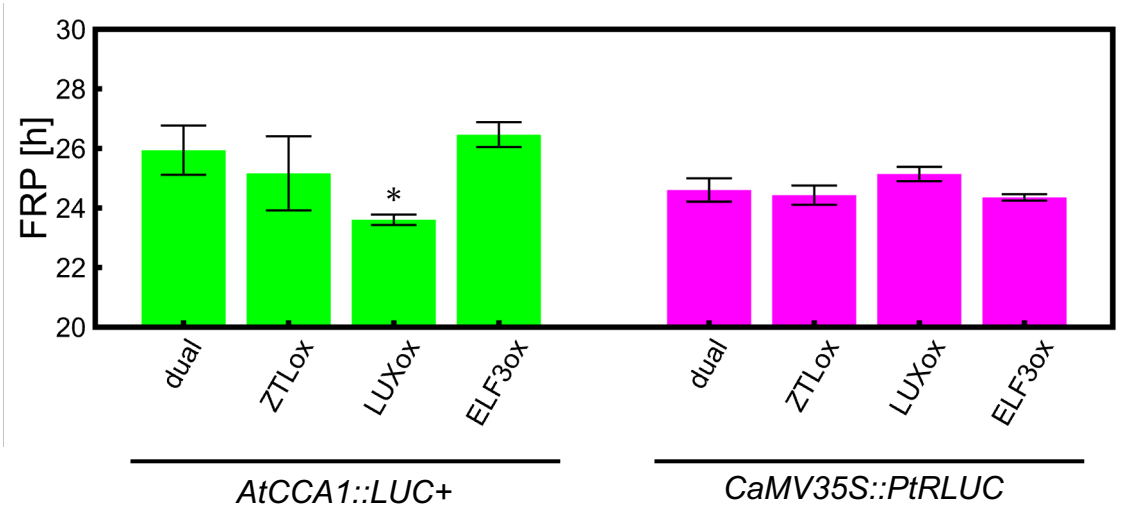

Figure S2. Free running periods (FRPs) of *AtCCA1::LUC+* and *CaMV35S::PtRLUC* bioluminescence rhythms in overexpression experiments
FRPs of cellular bioluminescence rhythms in the control (dual; dual#1-#4), *LmZTL* (ZTLox; dual-ZTLox#1-#3), *LmLUX* (LUXox; dual-LUXox#1-#3) and *LmELF3* (ELF3ox; dual-ELF3ox#1-#3) overexpression experiments. Data are expressed as mean ± SE. Asterisk denotes statistically significant difference (Welch's *t* test, $p < 0.05$).

Figure S3

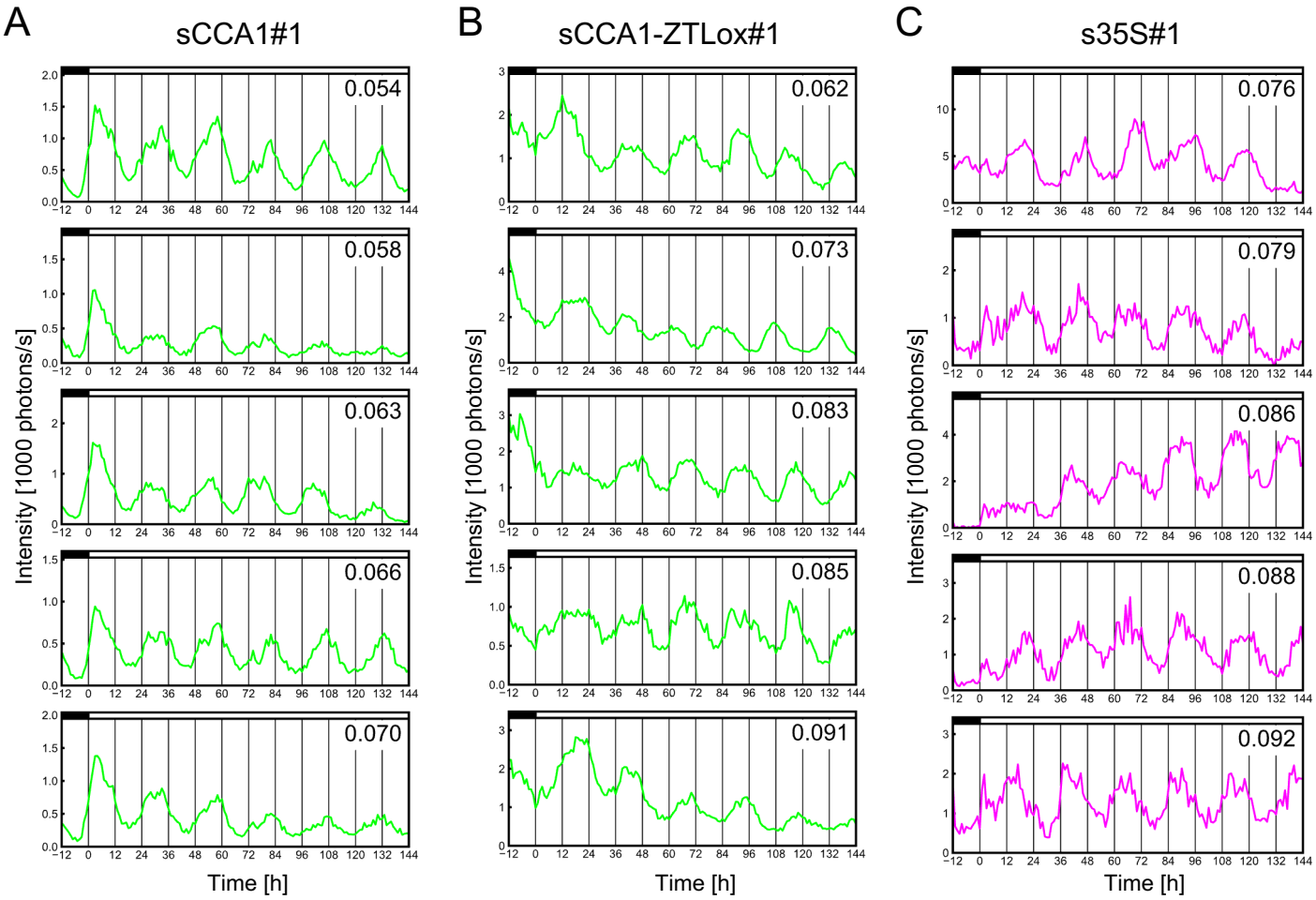

Figure S3. Cellular *AtCCA1::LUC*+ bioluminescence rhythms in an *LmZTL* overexpression experiment with single-reporter

Examples of bioluminescence rhythms of individual cells in single-reporter experiments: sCCA1#1 (A), sCCA1-ZTLox#1 (B), and s35S#1 (C). The cellular bioluminescence rhythms with the five lowest relative amplitude error (RAE) values in each experiment are shown in ascending order. The RAE is indicated in each graph. Close and open boxes represent light and dark conditions, respectively.

Figure S4

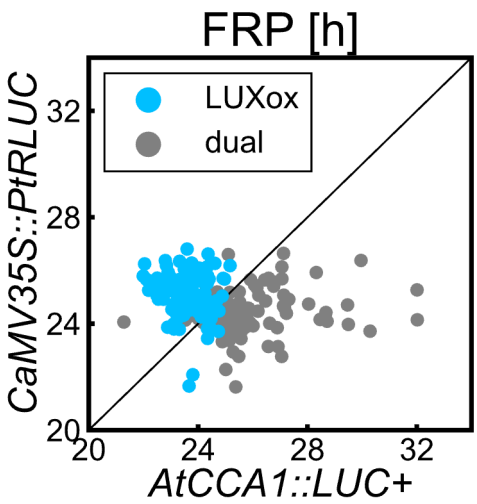

Figure S4. A scatterplot of the free-running periods (FRPs) between *AtCCA1::LUC+* and *CaMV35S::PtRLUC* rhythms in dual-reporter experiments with or without *CaMV35S::LmLUX*
FRPs of the 132 cells showing the circadian rhythms of both reporters in the three overexpression experiments (dual-LUXox#1-#3) are plotted with blue dots. FRPs of the 116 cells showing the circadian rhythms of both reporters in the four experiments without the effector (dual#1-#4) are plotted with gray dots (the same plots as those in Figure 3B). The dashed line represents where the FRPs are identical in both rhythms.

Figure S5

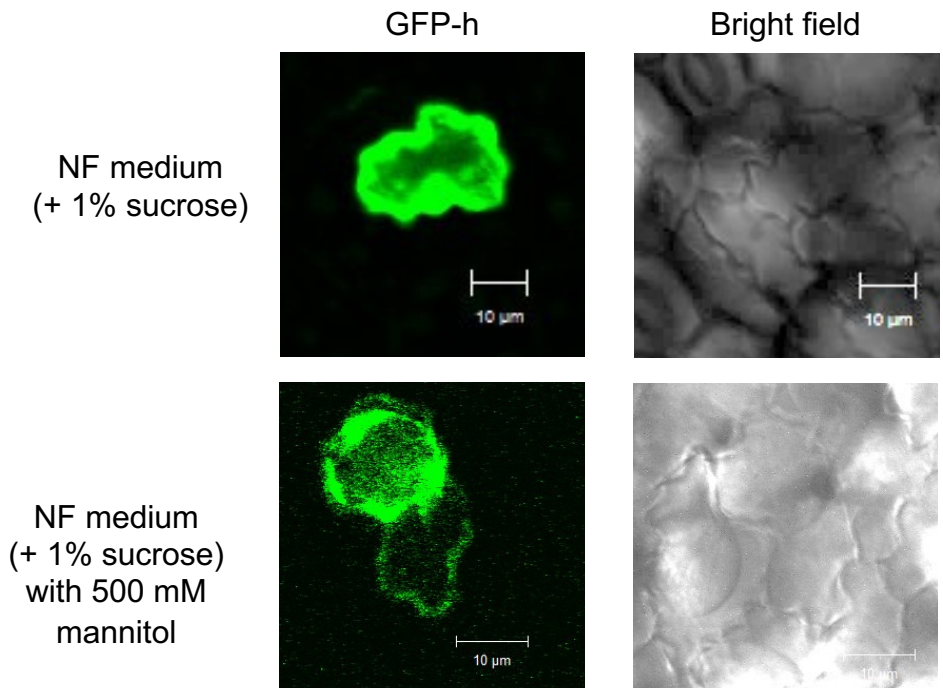

Figure S5. Plasmolysis of cells under hypertonic conditions
GFP fluorescence images of cells that were transfected with an endoplasmic reticulum (ER) localized GFP reporter (*CaMV35S::GFP-h*) and bright field images are shown. An epidermal cell of an *L. minor* plant in NF medium with 1% sucrose and that in NF medium with 1% sucrose and 500 mM mannitol are shown. Bars represent 10 μm.

Table S1. Summary of the quantitative analysis of cellular bioluminescence rhythms in dual reporter experiments

Experiment name	# Identified cells	# Analyzed cells	# Rhythmic in both reporters	*AtCCA1::LUC+*					*CaMV35S::PtRLUC*				
				# Rhythmic cells	Rhythmic ratio	FRP[1] [h]	Phase [rad]	SI	# Rhythmic cells	Rhythmic ratio	FRP[1] [h]	Phase [rad]	SI
dual#1	52	37	33	33	0.89	25.5 ± 0.8 (25.5 ± 0.8)	5.045	0.979	37	1	24.7 ± 0.6 (24.7 ± 0.6)	1.89	0.921
dual#2	61	54	50	50	0.93	25.6 ± 1.6 (25.6 ± 1.6)	4.977	0.986	54	1	24.0 ± 0.7 (24.0 ± 0.7)	0.334	0.919
dual#3	41	20	18	18	0.9	25.3 ± 1.4 (25.3 ± 1.4)	5.204	0.958	20	1	24.8 ± 0.7 (24.8 ± 0.8)	1.463	0.909
dual#4	35	17	15	15	0.88	27.4 ± 2.1 (27.4 ± 2.1)	4.307	0.926	17	1	25.0 ± 0.9 (25.0 ± 0.9)	1.495	0.878
dual-ZTLox#1	41	29	6	6	0.21	23.9 ± 1.3 (23.9 ± 1.3)	1.081	0.807	29	1	24.1 ± 0.6 (24.1 ± 0.4)	0.701	0.981
dual-ZTLox#2	24	10	3	3	0.3	26.9 ± 3.2 (26.9 ± 3.2)	2.678†	0.946†	10	1	24.4 ± 2.2 (24.5 ± 0.8)	1.767†	1†
dual-ZTLox#3	33	8	4	4	0.5	24.7 ± 1.0 (24.7 ± 1.0)	1.899	0.839	8	1	24.7 ± 0.3 (24.8 ± 0.4)	1.978	0.991
dual-LUXox#1	78	48	39	41	0.85	23.3 ± 0.7 (23.4 ± 0.7)	5.897	0.981	44	0.92	25.3 ± 0.5 (25.2 ± 0.5)	0.974	0.936
dual-LUXox#2	60	54	37	41	0.76	23.7 ± 0.7 (23.7 ± 0.6)	6.045	0.976	46	0.85	25.3 ± 0.9 (25.4 ± 0.9)	1.325	0.932
dual-LUXox#3	66	64	56	58	0.91	23.8 ± 0.6 (23.7 ± 0.6)	5.905	0.983	60	0.94	24.8 ± 0.7 (24.8 ± 0.7)	0.971	0.896
dual-ELF3ox#1	52	38	20	21	0.55	26.5 ± 1.7 (26.6 ± 1.7)	5.891	0.505	37	0.97	24.5 ± 2.2 (24.4 ± 2.9)	0.966	0.901
dual-ELF3ox#2	59	55	10	14	0.25	26.0 ± 1.4 (25.9 ± 1.2)	5.282	0.637	51	0.93	24.1 ± 1.1 (24.2 ± 1.4)	1.199	0.841
dual-ELF3ox#3	32	20	3	7	0.35	27.3 ± 1.6 (26.9 ± 1.3)	3.136	0.901	13	0.65	23.8 ± 0.8 (24.5 ± 0.4)	1.471†	0.957†
dual-hyper#1	37	36	0	33	0.92	28.2 ± 1.2 (N.A)	N.A	N.A	1	0.03	26.0 (N.A)	N.A	N.A
dual-hyper#2	32	13	0	6	0.46	28.1 ± 1.3 (N.A)	N.A	N.A	0	0	N.A (N.A)	N.A	N.A
dual-hyper#3	47	46	2	45	0.98	27.9 ± 1.1 (30.7 ± 2.0)	4.29†	1†	2	0.04	23.4 ± 0.4 (23.4 ± 0.4)	5.734†	1†
dual-hyper#4	26	18	0	15	0.83	27.9 ± 1.7 (N.A)	N.A	N.A	0	0	N.A (N.A)	N.A	N.A

[1]Mean FRP ± SD for the cells showing the circadian rhythm of the reporter (top), and for those showing the circadian rhythms of both reporters (bottom and in parentheses).
†The hypothesis that specifies a unique spread of directions in the unit circle is not rejected (Rayleigh test, $p > 0.01$).
N.A: Not applicable.

Table S2. Summary of the quantitative analysis of cellular bioluminescence rhythms in single reporter experiments

			AtCCA1::LUC+					*CaMV35S::PtRLUC*				
Experiment name	# Identified cells	# Analyzed cells	# Rhythmic cells	Rhythmic ratio	FRP[1] [h]	Phase [rad]	SI	# Rhythmic cells	Rhythmic ratio	FRP[1] [h]	Phase [rad]	SI
sCCA1#1	21	21	19	0.9	25.4 ± 1.3	5.558	0.865	-	-	-	-	-
sCCA1#2	43	42	42	1	24.6 ± 0.8	5.654	0.954	-	-	-	-	-
sCCA1#3	18	15	10	0.67	25.1 ± 1.0	5.284	0.983	-	-	-	-	-
s35S#1	29	22	-	-	-	-	-	19	0.86	23.4 ± 2.7	1.087	0.937
s35S#2	47	47	-	-	-	-	-	45	0.96	24.6 ± 0.5	0.706	0.905
s35S#3	53	52	-	-	-	-	-	50	0.96	24.7 ± 0.6	0.819	0.899
sCCA1-ZTLox#1	35	35	17	0.49	23.7 ± 2.4	1.847	0.819	-	-	-	-	-
sCCA1-ZTLox#2	33	33	22	0.67	24.5 ± 0.6	1.774	0.906	-	-	-	-	-
s35S-ZTLox#1	37	37	-	-	-	-	-	35	0.95	24.1 ± 0.7	0.384	0.886
s35S-ZTLox#2	38	38	-	-	-	-	-	36	0.95	24.7 ± 0.9	0.297	0.953
sCCA1-LUXox#1	34	32	31	0.97	23.6 ± 0.8	5.975	0.932	-	-	-	-	-
sCCA1-LUXox#2	26	23	21	0.91	23.6 ± 1.2	5.713	0.972	-	-	-	-	-
s35S-LUXox#1	51	51	-	-	-	-	-	51	1	24.6 ± 0.5	1.118	0.923
s35S-LUXox#2	44	44	-	-	-	-	-	41	0.93	25.0 ± 0.9	1.342	0.905
sCCA1-ELF3ox#1	37	37	25	0.68	27.0 ± 3.4	5.147	0.53	-	-	-	-	-
s35S-ELF3ox#1	57	56	-	-	-	-	-	55	0.98	22.8 ± 1.0	0.881	0.856
s35S-ELF3ox#2	68	68	-	-	-	-	-	53	0.78	22.3 ± 1.4	1.269	0.872

[1]Mean FRP ± SD for rhythmic cells.